

# HYPERSPECTRAL SIGNAL MODELS AND IMPLICATIONS TO MATERIAL DETECTION ALGORITHMS

*Dimitris Manolakis*

MIT Lincoln Laboratory  
244 Wood Street, Lexington, MA 02420-9185.  
E-mail: dmanolakis@ll.mit.edu

## ABSTRACT

The purpose of this paper is to present a concise overview of hyperspectral signal models and the target detection algorithms resulting from their adoption. We focus on detection algorithms derived using established statistical techniques and whose performance is predictable under reasonable assumptions about hyperspectral imaging data. We show that the family of elliptically contoured distributions (ECDs), in general, and the t-ECD, in particular, provide a more accurate model for hyperspectral backgrounds, compared to the widely used multivariate normal distribution. Since many detection algorithms derived for normal distributions apply to ECDs as well, the ECD models provide a better framework for modeling and analyzing hyperspectral imaging data.

## 1. INTRODUCTION

The detection of materials and objects using remotely sensed spectral information has many military and civilian applications. Hyperspectral imaging sensors measure the radiance for every pixel at a large number ( $K$ ) of narrow spectral bands. The obtained measurements, arranged as a column vector  $\mathbf{x}$ , are known as the radiance spectrum of the pixel. In the reflective part of the electromagnetic spectrum ( $0.4\mu\text{m}$ - $2.5\mu\text{m}$ ), the spectral information characterizing a material is the reflectance spectrum, defined as the ratio between reflected and incident radiation as a function of wavelength.

We focus on detection algorithms that exploit spectral information, only. Target detection algorithms for hyperspectral imaging data, can be grouped into two types: Spectral matching algorithms, which require spectral information about the targets of interest, and anomaly detection algorithms which do *not* require knowledge of the spectral signatures of the targets of interest.

The task of a target detection algorithm is to decide, by means of a statistical hypothesis test, whether a target of in-

This work was sponsored by the Department of the Defense under Air Force contract F19628-00-C-0002. Opinions, interpretations, conclusions, and recommendations are those of the author and not necessarily endorsed by the United States Government.

terest is present or not present in a pixel-under-test (PUT) with observed spectrum  $\mathbf{x}$ . We typically use a binary hypothesis test to choose between the following competing null and alternative hypotheses:  $H_0$ : Target absent and  $H_1$ : Target present. According to the Neyman-Pearson (NP) criterion, the optimum decision strategy (maximize the probability of detection  $P_D$  while keep the probability of false alarm  $P_{FA}$  under a certain value) is given by the likelihood ratio test (LRT):  $\Lambda(\mathbf{x}) = \frac{f_1(\mathbf{x}|H_1)}{f_0(\mathbf{x}|H_0)} \underset{H_0}{\overset{H_1}{\geq}} \eta$ , where  $f_0(\mathbf{x}|H_0)$  and

$f_1(\mathbf{x}|H_1)$  are the probability density functions (pdfs) of the observed data vector under the two hypotheses. The decision threshold  $\eta$  is set to yield the desired probability of false alarm  $P_{FA}$  [1]. The main objective of this paper is to provide a concise review of some widely used HSI signal models and the resulting detection algorithms. This discussion expands and complements the work presented in [2, 3].

## 2. HYPERSPECTRAL SIGNAL MODELS

Under the  $H_0$  hypothesis, the PUT consists only of background. Under the  $H_1$  hypothesis, depended on the relative sizes of the target and the ground resolution cell, the PUT may consist of only target or target and background. When the PUT is filled with the target, we talk about resolved or full-pixel targets. When only part of the pixel is filled with the target, we talk about unresolved or sub-pixel targets. In this case, essentially, the target *replaces* part of the background in the PUT. If we denote by  $\mathbf{s}$  the spectrum of the target, and by  $\mathbf{v}$  the spectrum of the background, and by  $\alpha \geq 0$  the fraction of the PUT area filled by the target, the observed spectrum is

$$\mathbf{x} = \alpha\mathbf{s} + (1 - \alpha)\mathbf{v} \quad (1)$$

which is known as the *replacement signal model* for sub-pixel targets. The replacement model can be approximated by a linear signal model if  $\alpha \ll 1$  ( $\Rightarrow \mathbf{x} \approx \alpha\mathbf{s} + \mathbf{v}$ ) or  $\alpha \approx 1$  ( $\Rightarrow \mathbf{x} \approx \mathbf{s} + (1 - \alpha)\mathbf{v}$ ). Although the replacement model makes better sense for sub-pixel targets, for mathematical

simplicity we use the following linear model

$$\mathbf{x} = \alpha \mathbf{s} + \beta \mathbf{v} \quad (2)$$

where  $\alpha$  and  $\beta$  can take any values, positive or negative.

## 2.1. Background Modeling

The most widely used background model assumes that  $\mathbf{v}$  is a random vector with a multivariate normal (or Gaussian) pdf given by

$$f(\mathbf{v}) = \frac{1}{(2\pi)^{K/2} |\mathbf{\Gamma}|^{1/2}} \exp \left[ -\frac{1}{2} (\mathbf{v} - \boldsymbol{\mu})^T \mathbf{\Gamma}^{-1} (\mathbf{v} - \boldsymbol{\mu}) \right] \quad (3)$$

where  $\boldsymbol{\mu} = E(\mathbf{v})$  is the mean vector,  $\mathbf{\Gamma} = E[(\mathbf{v} - \boldsymbol{\mu})(\mathbf{v} - \boldsymbol{\mu})^T]$  is the covariance matrix, and  $|\cdot|$  denotes matrix determinant. In shorthand notation  $\mathbf{v} \sim N(\boldsymbol{\mu}, \mathbf{\Gamma})$  or equivalently  $g(\mathbf{v}; \boldsymbol{\mu}, \mathbf{\Gamma})$ . The quadratic expression

$$\Delta^2(\mathbf{v}, \boldsymbol{\mu}; \mathbf{\Gamma}) = (\mathbf{v} - \boldsymbol{\mu})^T \mathbf{\Gamma}^{-1} (\mathbf{v} - \boldsymbol{\mu}) \quad (4)$$

is a widely used statistical distance measure, known as the *Mahalanobis distance*. It can be shown that if  $\mathbf{v} \sim N(\boldsymbol{\mu}, \mathbf{\Gamma})$ , then  $\Delta^2 \sim \chi_K^2$  (chi-squared distribution with  $K$  degrees of freedom). A more accurate statistical model for hyperspectral backgrounds [4, 5], is the multivariate elliptically contoured (EC)  $t$ -distribution given by

$$t_K(\mathbf{v}; \boldsymbol{\mu}, \mathbf{C}, M) = \frac{\Gamma[(K+M)/2]}{\Gamma(M/2)(M\mathbf{C})^{K/2} |\mathbf{C}|^{1/2}} \times \left[ 1 + \frac{1}{M} (\mathbf{v} - \boldsymbol{\mu})^T \mathbf{C}^{-1} (\mathbf{v} - \boldsymbol{\mu}) \right]^{-\frac{K+M}{2}} \quad (5)$$

where  $M$  is the number of degrees of freedom,  $\mathbf{C} = (1 - 2/M)\mathbf{\Gamma}$  is the *scale* matrix, and  $\Gamma(\cdot)$  denotes the gamma function. The Mahalanobis distance is distributed as

$$\frac{1}{K} (\mathbf{v} - \boldsymbol{\mu})^T \mathbf{C}^{-1} (\mathbf{v} - \boldsymbol{\mu}) \sim F_{K,M} \quad (6)$$

where  $F_{K,M}$  is the F-distribution with  $K$  and  $M$  degrees of freedom. The integer  $M$  controls the tails of the distribution:  $M = 1$  leads to the multivariate Cauchy distribution (heavier tails), whereas as  $M \rightarrow \infty$  the EC  $t$ -distribution approaches the multivariate normal distribution (lighter tails).

The empirical distribution of the Mahalanobis distance of a hyperspectral data cube, can be used to identify its joint spectral distribution by comparing to the theoretical chi-squared and F-distributions corresponding to the multivariate normal and  $t$ -distributions. In examining the statistical properties of the data, several groupings, or classes, were considered. Three regions are identified in the white boxes in Figure 1 describing three classes that were selected by their

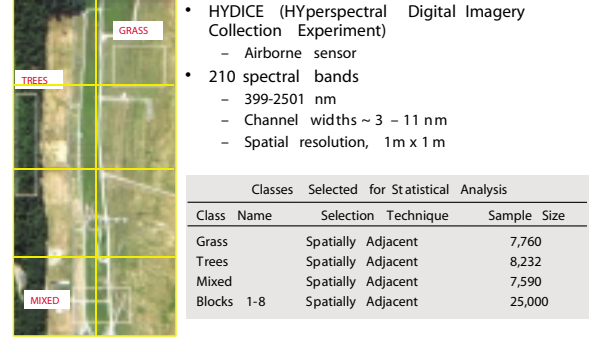


**Fig. 1.** Division of data cube into rectangular blocks to reduce spatial inhomogeneity.

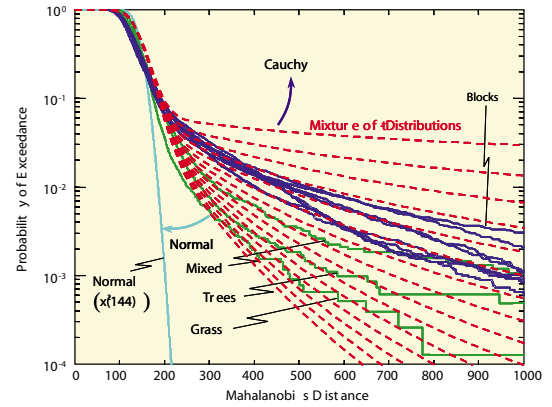


**Fig. 2.** Modelling the distribution of the Mahalanobis distance for the HSI data blocks shown in Figure 1.

spatial proximity. In the lower right is a "Grass" region, the middle top is a "Tree" region, and on the left is a "mixed" region. These regions define the pixels selected for three of the classes considered. Also considered were two classes resulting from a supervised classification process performed to isolate spectrally similar (not necessarily spatially adjacent) pixels. To reduce the effects of spatial inhomogeneity, we divide the data cube into rectangular blocks as shown in Figure 1. The distribution of the Mahalanobis distance is shown in Figure 2 for all blocks plus the three spatially determined classes.

Another way to reduce spatial inhomogeneity is to model each class obtained by supervised or unsupervised classification separately. To this end, we use the classes shown in Figure 3, which have been derived by elaborate processing techniques by a group at the Remote Sensing Laboratory, Purdue University. The distribution of the Mahalanobis distance for the five most populated classes is shown in Figure 4. The results in Figures 2 and 4 indicate that the EC  $t$ -distribution provides a promising model for HSI data. We note that the  $t$ -distribution tends to the normal distribution

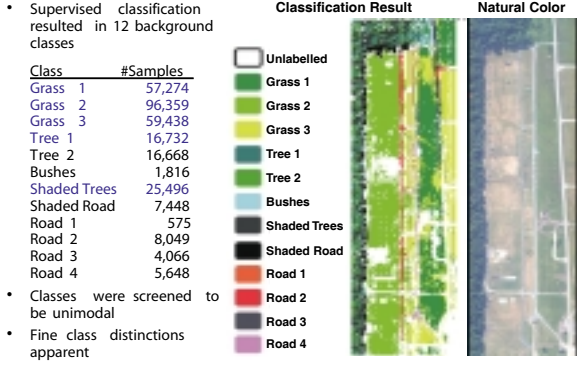


**Fig. 3.** Classes, classification results, and natural color image for the analyzed HYDICE data cube.

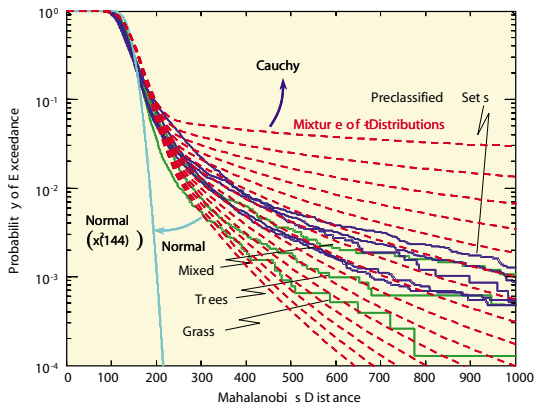


**Fig. 4.** Modelling the distribution of the Mahalanobis distance of the HSI data classes shown in Figure 3.

when the number of degrees of freedom increases.

## 2.2. Target Modeling

In contrast to the background, the target spectrum  $s$  is usually model by a multivariate normal distribution  $s \sim N(\mu_s, \Gamma_s)$ . Because the tails of the distribution do not significantly affect the probability of detection, there is no need to use the more complicated ECD models. It can be shown that this random signal model is equivalent to the so-called Gaussian linear model  $s = H\theta$ ,  $\theta \sim N(\mu_\theta, \sigma_\theta^2 I_P)$ , where  $H(K \times P)$  is the mode matrix and the elements of  $\theta(P \times 1)$  are the mode weights ( $P \leq K$ ). According to this model, the target  $s$  lies in the linear subspace spanned by the columns of  $H$ , but its location is unknown because  $\theta$  is unknown. The spectrum vector can be placed randomly or deterministically in an unknown location of a known subspace. Most detection algorithms have been derived using a deterministic placement. However, a remarkable result developed in [6] shows that the subspace detectors for known covariance matrix are GLRT for both deterministic and stochastic subspace signals.

## 3. MATERIAL DETECTION ALGORITHMS

Figure 5 shows a taxonomy of a variety of algorithms for hyperspectral target detection. A detailed discussion of these algorithms from a hyperspectral image processing perspective is provided in [2, 3], whereas a theoretical analysis of the subspace detection algorithms is given in [7]. Figures 6 and 7 illustrate the performance of different detection algorithms for three materials with different spectral signatures. The lack of a large number of target pixels makes difficult the generation of reliable receiver operating characteristic (ROC) curves; more details can be found in [3].

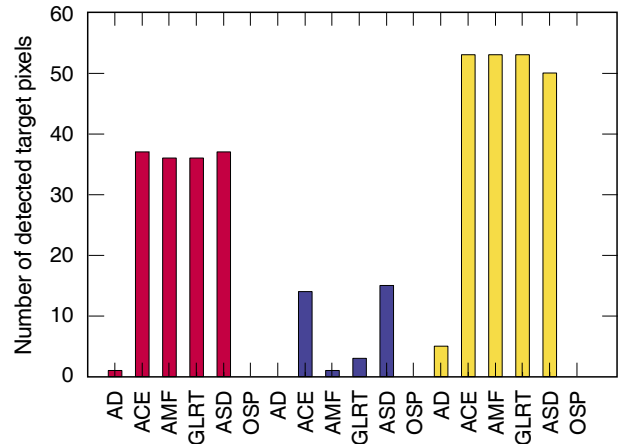


**Fig. 6.** Summary of detection performance of the various detectors for three different target signatures. Each bar shows the number of detected targets for a  $10^{-4}$  probability of false alarm.

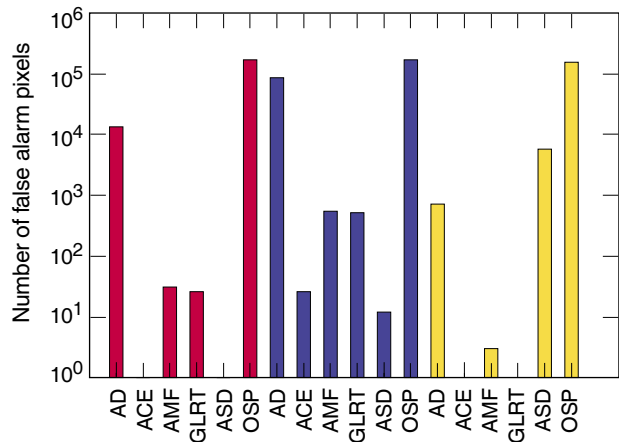


**Fig. 7.** Summary of detection performance of the various detectors for three different target signatures. Each bar shows the probability of false alarm for a threshold that assures the detection of all full-pixel targets.

	Signal Model	Assumptions	Detector $y = D(\mathbf{x})$	Name	Comments	
Target Resolution	Full pixel targets	$H_0: \mathbf{x} \sim N(\mu_b, \Gamma_b)$ $H_1: \mathbf{x} \sim N(\mu_t, \Gamma_t)$	Known $\mu_b, \mu_t, \Gamma_b, \Gamma_t$	$(\mathbf{x} - \mu_b)^T \Gamma_b^{-1} (\mathbf{x} - \mu_b) -$ $(\mathbf{x} - \mu_t)^T \Gamma_t^{-1} (\mathbf{x} - \mu_t)$	Bayes or Neyman-Pearson quadratic classifiers	$\Gamma \triangleq \Gamma_t = \Gamma_b \Rightarrow$ $y = (\mu_t - \mu_b)^T \Gamma^{-1} \mathbf{x}$ Plug-in detectors: estimate $\mu_t, \mu_b, \Gamma_t, \Gamma_b$ from training data
		Training data for $\mu_b, \Gamma_b$ only	$(\mathbf{x} - \hat{\mu})^T \hat{\Gamma}^{-1} (\mathbf{x} - \hat{\mu})$	Mahalanobis distance	Anomaly detection RX algorithm CFAR	
	Subpixel targets	$H_0: \mathbf{x} = \mathbf{b}$ $H_1: \mathbf{x} = \mathbf{S}\mathbf{a} + \sigma\mathbf{b}$ $\mathbf{S}$ known ( $L \times P$ ) matrix $H_0: \mathbf{x} \sim N(\mathbf{0}, \Gamma)$ $H_1: \mathbf{x} \sim N(\mathbf{S}\mathbf{a}, \sigma^2 \Gamma)$	Training data under $H_0: \mathbf{x}(1), \mathbf{x}(2), \dots, \mathbf{x}(N)$ $\hat{\mu} = \frac{1}{N} \sum_{n=1}^N \mathbf{x}(n)$ $\hat{\Gamma} = \frac{1}{N} \sum_{n=1}^N [\mathbf{x}(n) - \hat{\mu}][\mathbf{x}(n) - \hat{\mu}]^T$	$\frac{\mathbf{x}^T \hat{\Gamma}^{-1} \mathbf{S} (\mathbf{S}^T \hat{\Gamma}^{-1} \mathbf{S})^{-1} \mathbf{S}^T \hat{\Gamma}^{-1} \mathbf{x}}{\psi_1 + \psi_2 \mathbf{x}^T \hat{\Gamma}^{-1} \mathbf{x}}$	Name $\psi_1$ $\psi_2$ $\sigma$ Kelly $N$ 1 1 AMF 1 0 1 ACE 0 1 ? ? = unknown	CFAR $\text{SINR}_0 = (\mathbf{S}\mathbf{a}_1)^T \Gamma^{-1} (\mathbf{S}\mathbf{a}_1)$ $y = \mathbf{x}^T \hat{\Gamma}^{-1} \mathbf{x}$ (Matched filter)
		$P=1 \Rightarrow S \rightarrow s$	$\frac{s^T \hat{\Gamma}^{-1} \mathbf{x}}{(s^T \hat{\Gamma}^{-1} s)^{1/2} (\psi_1 + \psi_2 \mathbf{x}^T \hat{\Gamma}^{-1} \mathbf{x})^{1/2}}$	AMF = Adaptive Matched Filter ACE = Adaptive Cosine/Coherence Estimator	Low-rank covariance matrix approximation: $\hat{\Gamma} \approx \sum_{k=1}^Q \lambda_k \mathbf{u}_k \mathbf{u}_k^T \Rightarrow \hat{\Gamma}^{-1} \approx \sum_{k=1}^Q \frac{1}{\lambda_k} \mathbf{u}_k \mathbf{u}_k^T$	
		$H_0: \mathbf{x} = \mathbf{B}\mathbf{a}_b + \mathbf{w}$ $H_1: \mathbf{x} = \mathbf{S}\mathbf{a}_t + \mathbf{B}\mathbf{a}_b + \mathbf{w}$	$\mathbf{w} \sim N(\mathbf{0}, \sigma_w^2 \mathbf{I})$ $\mathbf{Z} \triangleq [\mathbf{S} \ \mathbf{B}]$ $\mathbf{P}_A^\perp \triangleq \mathbf{I} - \mathbf{A}(\mathbf{A}^T \mathbf{A})^{-1} \mathbf{A}^T$	$\frac{\mathbf{x}^T (\mathbf{P}_B^\perp - \mathbf{P}_Z^\perp) \mathbf{x}}{\mathbf{x}^T \mathbf{P}_Z^\perp \mathbf{x}}$	GLRT detector	CFAR $\text{SINR}_0 = \frac{\ \mathbf{P}_B^\perp \mathbf{S}\mathbf{a}_t\ }{\sigma_w^2}$
				$s \mathbf{P}_B^\perp \mathbf{x}$	Orthogonal subspace projector (OSP)	Non CFAR

Fig. 5. Taxonomy of hyperspectral imaging target detection algorithms.

#### 4. CONCLUSIONS

In this paper, we presented a unified view of hyperspectral signal models and resulting detection algorithms from a signal processing perspective. An important property of some of the discussed algorithms (GLRT, ACE, AMF) is that they preserve their structure, which was obtained for normally distributed backgrounds, for the more general class of ECDs [8]. Although the theoretical properties and performance for the additive signal model have been extensively studied, a similar investigation for the replacement model is not available.

#### 5. REFERENCES

- [1] S. M. Kay, *Fundamentals of Statistical Signal Processing*, Prentice Hall, New Jersey, 1998.
- [2] Dimitris Manolakis and Gary Shaw, "Detection algorithms for hyperspectral imaging application," *IEEE Signal Processing Magazine*, pp. 29–43, January 2002.
- [3] Dimitris Manolakis, David Marden, and Gary Shaw, "Target detection algorithms for hyperspectral imaging application," *Lincoln Laboratory Journal*, vol. 14, no. 1, pp. 79–116, 2003.
- [4] Dimitris Manolakis and David Marden, "Non gaussian models for hyperspectral algorithm design and assessment," in *IEEE International Geoscience and Remote Sensing Symposium*. June 2002, pp. 1664–1666, IEEE.
- [5] David Marden and Dimitris Manolakis, "Modeling hyperspectral imaging data using elliptically contoured distributions," in *Algorithms and Technologies for Multi-spectral, Hyperspectral, and Ultraspectral Imagery IX*, Sylvia S. Shen and Paul E. Lewis, Eds., Orlando, FL, 2003, SPIE.
- [6] Todd McWhorter and Louis L. Scharf, "Matched subspace detectors for stochastic signals," in *The 11th Annual Workshop on Adaptive Sensor Array Processing*. March 2003, MIT Lincoln Lab.
- [7] S. Kraut, L.L. Scharf, and L. T. McWhorter, "Adaptive subspace detectors," *IEEE Transactions on Signal Processing*, vol. 49, no. 1, pp. 1–16, January 2001.
- [8] Christ D. Richmond, *Adaptive Array Signal Processing and Performance Analysis in Non-Gaussian Environments*, Doctor of philosophy, Massachusetts Institute of Technology, Cambridge, MA, May 1996.